Characterization and Selection of Probability Statistical Parameters in Random Slope PWM Based on Uniform Distribution

Jie Xu, Ziling Nie, and Junjie Zhu, *Member, IEEE*

***Abstract*—To deal with the uncertain relationship between random variables and harmonic spectrum in existing random pulsewidth modulation (PWM), this article links the uniformly distributed random carrier sequence probabilistic parameters with harmonic distributed in the frequency domain, offers an approach to selecting a random carrier sequence. Based on random slope PWM, the formula for 3-dB bandwidth of harmonic power spectrum is deduced. Then, some useful conclusions are also drawn under random carrier sequence obeying uniform distribution. The 3-dB bandwidth formula leads to a method of selecting the main probability statistical parameters. The method has laid a theoretical foundation for the design and selection of random variables in random PWM, provided a scientific reference for the study of random PWM technology, which is used to reduce electromagnetic interference and mechanical vibration.**

***Index Terms*—3-dB bandwidth of harmonic power spectrum, probability statistical parameters, random carrier sequence, random slope pulsewidth modulation (PWM), uniform distribution.**

I. Introduction

THE pulsewidth modulation (PWM) with fixed switching frequency has wide application in power electronic technology. However, its output harmonic peaks appearing at switching frequency and its multiple frequencies will cause damage, which worthy of attention [1].

For the power system, harmonic peaks are the main cause of electromagnetic interference (EMI). In terms of load, the harmonic peaks not only cause mechanical vibration, which can shorten the service life of equipment but also produce a certain amount of acoustic vibration, or noise contamination [2], [3].

To suppress EMI and vibration, filters, and dampers are usually used. However, they have some disadvantages. For example, the cost of the active filter is high and its harmonic detection and compensation are complex. And the passive filters are slow in dynamic response and poor in filtering effect during the fast-changing process. Besides, added devices take up a lot of space and increase the overall weight of the equipment. Therefore, these methods are not ideal solutions.

In 1990s, Trzynadlowski [5] proposed a random PWM based on the control of the ON-OFF of switching devices to change the duty ratio. He and his team members thought that if carrier sequence was random enough, its random degree would be very high and the harmonic peaks would be scattered to other frequency points. In ideal conditions, the harmonic spectrum could come close to white noise.

In random PWM, it is essential to use a random function. Because of the nonexistence of its Fourier transform, the random function is difficult to use directly for frequency- domain analysis. As there is research overlapping among random PWM, such as random signal analysis, vibration noise treatment, and more difficulties appear in the article, which makes it hard to deeply understand the mechanism of harmonic dispersion. Later, Trzynadlowski and his team proposed the random PWM of "harmonic-frequency-spectrum null point". Compared with fixed carrier PWM (FCPWM), the technology could decrease EMI by more than 10 dB under the same experimental conditions [6], [7]. The contribution made in this study has brought about a new research topic. However, the modeling and theoretical analyses of random PWM are not much different from the previous study.

The study's authors made a comparative analysis of the relationship between random carrier frequency (RCS) distribution and output voltage harmonic frequency domain distribution. The conclusion is that the former has little effect on the later [8]. Researchers also studied the upper and lower limits of RCS by experiments and found the law of output voltage harmonic spectrum when modulation wave is four or five times as large [9]. In the application of a uniform random number, some researchers introduced the Markov chain based on FCPWM. It enables random PWM periodic values to be more evenly distributed around expected values, thereby making the spectrum of output current more uniform [11], [12]. It is not clear whether RCS can realize the best uniform distribution or not. Some optimization algorithm does not show the principles of random PWM [13], [14]. This problem needs to be further studied yet.

In present researches, the increase of harmonic dispersion in the frequency domain mostly depends on improving random PWM by changing random strategy and increasing random degree of random variables. But there has not been yet an established standard to judge how the stochastic degree is depending

Manuscript received January 26, 2020; revised April 10, 2020 and May 26, 2020; accepted June 21, 2020. Date of publication June 23, 2020; date of current version September 4, 2020. This work was supported by the National Natural Science Foundation of China under Grant 51807199. Recommended for publication by Associate Editor Prof. S. K. Mazumder. *(Corresponding author: Ziling Nie.)*

The authors are with the Specialized Electrical Research Institute of Science and Technology, Naval University of Engineering, Wuhan 430033, China (e-mail: baboo_x@163.com; 794132048@qq.com; 543052377@qq.com).

Color versions of one or more of the figures in this article are available online at https://ieeexplore.ieee.org.

Digital Object Identifier 10.1109/TPEL.2020.3004725

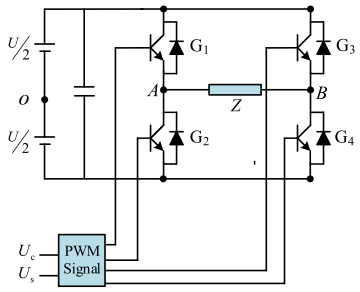

Fig. 1. Single-phase H-Bridge circuit topology.

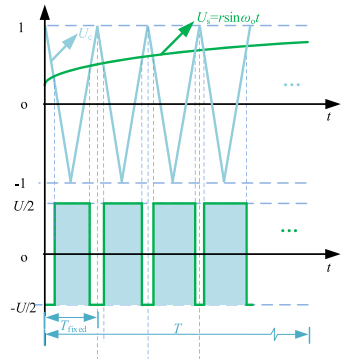

Fig. 2. Fixed carrier PWM.

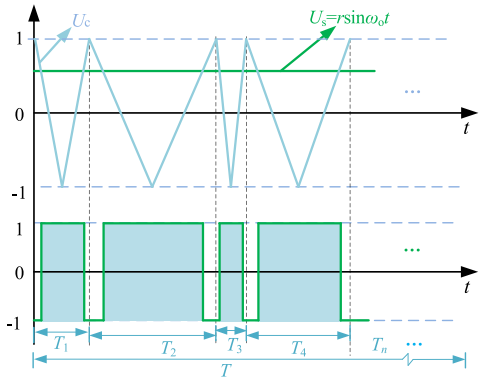

Fig. 3. Random slope PWM.

on diverse random strategies [15]–[18]. Random PWM spectrum analysis is another problem. As for FCPWM, [19] provides a 3-level, double-edge, sinusoidally modulated PWM wave using natural sampling. Song and Sarwate [20] gave expressions for the spectra of uniform-sampling PWM and natural sampling PWM signals. Based on the relationship between current THD and switching period rms in random PWM, the advice about current ripple reduction has been presented [21]–[26]. There is no doubt that a proper variable frequency PWM can attenuate the switching-related energy in certain frequency spectrum parts achieving acoustic noise and EMI reduction [27]–[31].

To solve the abovementioned problems, this article presents a random PWM technology. Detailed exploration such as random PWM harmonic distribution and carrier selection have also been done. Combined with engineering applications, studies will lay the solid foundation for selecting random functions and designing random variables in random PWM and can provide a theoretical basis for applying random PWM technology.

II. Random Slope PWM Based on Uniform Distribution

To analyze the relationship between the statistical parameters of RCS and harmonics distribution in the frequency domain, this section gives an introduction about the random slope PWM (RSPWM) model and then makes a detailed description of harmonic for the analysis of harmonic distribution in the frequency domain.

A. Model of Random Slope PWM

The single-phase H-bridge circuit topology is shown in Fig. 1. U, U_c, and U_s denote the input voltage of the dc terminal, the fixed-frequency carrier sequence, and the modulation wave, respectively. When the switches G_1 and G_4 are turned ON, the output voltage U_{AB} is $+U$. When G_2 and G_3 are turned ON, the output voltage U_{AB} is $-U$.

In Figs. 2 and 3, U_c is a carrier sequence, U_s is a modulation wave, ω_o is modulation wave angular frequency, T_c is fixed carrier period, and T_i is the i_{th} carrier period (corresponding to the carrier frequency f_i). When every random carrier period is the same, Fig. 2 shows FCPWM. When it is not the same, what is shown in Fig. 3 is referred to as RSPWM.

The number of random carriers is n, RCS can be expressed as $\{T_1, T_2, \ldots, T_n\}$. To keep total switching losses in RSPWM the same as that in FCPWM, the pulse number n, and average frequency f_{av} of RSPWM keep the same as that in FCWM during a repeating random period T.

When symmetrical regular sampling is used, the output voltage of FCPWM is expressed [32]–[35]

$$\begin{aligned}\frac{U(t)}{U/2} &= r\sin\omega_o t + \sum_{n=1}^{\infty}\left(\frac{4}{n\pi}\right)\sin\left[\frac{n\pi r\sin(\omega_o t)}{2}+\frac{n\pi}{2}\right]\\ &\quad\times\cos(n\omega_c t)\\ &= r\sin\omega_o t - \sum_{n=1}^{\infty}\left(\frac{4}{n\pi}\right)\cos\left[\frac{n\pi r\sin\omega_o t}{2}+\frac{(n-1)\pi}{2}\right]\\ &\quad\times\cos(n\omega_c t) \qquad (1)\end{aligned}$$

where ω_o is the modulation wave angular frequency, ω_c is the angular frequency of the carrier. The precondition of (1) is $\omega_c >> \omega_o$. Because the average frequency of the carrier is much larger than modulating wave frequency in RSPWM, the average symmetric regular sampling can also be used to analyze the harmonics spectrum of RSPWM.

However, it is hard to give an accurate expression of the output voltage in random PWM. With the view of the factorization, there is a phase difference between the fixed carrier PWM and

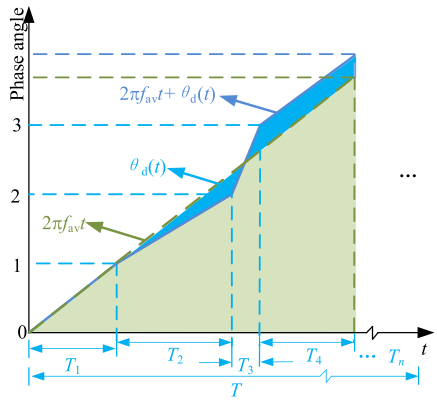

Fig. 4. Phase difference between FCPWM and RSPWM.

random carrier PWM for each n. Let c be the item including ω_o. When $n = 1$, the component contains carrier frequency, in (1) can be written as follows:

$$\begin{aligned}\frac{U(t)}{U/2} &= -\frac{4}{\pi}\cos\left(\frac{\pi c}{2}\right)\cos(\omega_c t)\\ &= -\frac{4}{\pi}\cos\left(\frac{\pi c}{2}\right)\cos(2\pi f_c t)\end{aligned} \tag{2}$$

where f_c is the frequency of the carrier. Similarly, the component indicates the random carrier sequence in the random PWM is

$$\frac{U_h(t)}{U/2} = -\frac{4}{\pi}\cos\frac{\pi c}{2}\cos[2\pi f_{\text{av}} t + \theta_{d1}(t)] \tag{3}$$

where f_{av} is the average frequency of the random carrier sequence. $\theta_{d1}(t)$ represents the phase difference between FCPWM and RSPWM when $n = 1$. $U_h(t)$ is the component of harmonics in RSPWM. $\theta_d(t)$ is the total phase difference between FCPWM and RSPWM, which is a function of time.

The statistical parameters of the random carrier sequence are the key to the settlement of the self-correlation function and power spectrum of the output voltage. From (3), it is known that the direct use of random carrier sequence to calculate the self-correlation function of $U_{h1}(t)$ is difficult. To establish the connection between random carrier sequence and phase difference, the random carrier sequence needs to be placed as $\{T_1, T_2, \ldots, T_n\}$, and each carrier corresponds to a single period. Taken $n = 1$ for example. The deduction of self-correlation and power spectrum functions has been shown as follows.

The phase difference between FCPWM and RSPWM can be described in Fig. 4.

In Fig. 4, the green line is angle variation of FCPWM, the carrier frequency value of which is the same as f_{av}. And the blue line stands for angle variation of RSPWM. The zone between the green line and the blue line is angle difference θ_d. Because of the randomness of θ_d, statistical parameters of phase difference are difficult to describe quantitatively. But statistical parameters of the phase difference can be set in advance. Based on the relationship between carrier and phase, the statistical parameters of the phase difference can be calculated. The detailed deduction is as follows.

The average value of RCS is expressed as

$$\overline{T} = \frac{1}{n}(T_1 + T_2 + \cdots + T_n). \tag{4}$$

The item in $\{T_1', T_2', T_3', \ldots, T_n'\}$ is defined as

$$T_i' = \left(T_1 + \cdots + T_i - i \times \overline{T}\right). \tag{5}$$

The basic relationship between each phase difference and carrier difference is

$$\theta_{di} = 2\pi f_{\text{av}} T_i'. \tag{6}$$

The variance of θ_{di} sequence θ_o^2 is determined as

$$\left(\left\lfloor\frac{n+1}{2}\right\rfloor\right)\frac{\theta_o^2}{4\pi^2 f_{\text{av}}^2} = E\left[\sum_{i=1}^{\lfloor\frac{n+1}{2}\rfloor}\left(T_1 + \cdots + T_i - i\overline{T}\right)^2\right]. \tag{7}$$

Because the carries in RCS are unrelated, θ_o^2 can be expressed in

$$\begin{aligned}\theta_o^2 &= \frac{\sum_{i=1}^{\lfloor n+1/2\rfloor}(i - \frac{i^2}{n})\times T_o^2}{\lfloor n+1/2\rfloor} \times 4\pi^2 f_{\text{av}}^2\\ &= \frac{(n+2)(2n-1)}{24\lfloor n+1/2\rfloor} \times 4\pi^2 f_{\text{av}}^2 T_o^2\\ &\approx \frac{2n\pi^2 f_{\text{av}}^2 T_o^2}{3}\end{aligned} \tag{8}$$

where T_o^2 is the variance of RCS $\{T_1, T_2, \ldots, T_n\}$. T_o^2 can be calculated by RCS. And T_o^2 is a fixed value.

The self-correlation function of θ_{di} at l intervals can be obtained from its expectation and the second-order center distance is

$$R_l(\theta_{dl}) = 1 - \frac{E[(\theta_{di} - \theta_{di+l})^2] - E^2[(\theta_{di} - \theta_{di+l})]}{2\theta_o^2} \tag{9}$$

where the expectation of θ_{di} is approximate to zero, and the second-order center distance of θ_{di} is

$$\begin{aligned}E[(\theta_{di} - \theta_{di+l})^2] &= E\{[(T_1 + T_2 + \cdots + T_i - i\overline{T})\\ &\quad - (T_1 + T_2 + \cdots + T_{i+l}) + (l+i)\overline{T}]^2\} \times 4\pi^2 f_{\text{av}}^2\\ &= E[(T_{i+1} + T_{i+2} + \cdots + T_{i+l}) - l\overline{T})^2] \times 4\pi^2 f_{\text{av}}^2\\ &= (l - l^2/n)T_o^2 \times 4\pi^2 f_{\text{av}}^2.\end{aligned} \tag{10}$$

According to (8), (9), and (10), the self-correlation function of θ_{di} at any interval l is expressed as

$$R(l) = 1 - \frac{3l(n-l)}{n^2}. \tag{11}$$

When there are n periods in a repeated random carrier cycle T, the expression is

$$n = \frac{T}{T_{\rm av}} = Tf_{\rm av}. \tag{12}$$

Similarly, the self-correlation function $\rho(\varepsilon)$ of the randomly changing phase θ_r at an interval ε is expressed as

$$\rho(\varepsilon) = 1 - \frac{3\,|\varepsilon|}{T} + \frac{3\varepsilon^2}{T^2}. \tag{13}$$

The variance of θ_{di} can be obtained from (8) and (12). It is expressed as

$$\theta_o^2 = \frac{2\pi^2 f_{\rm av}^3 T}{3} T_o^2. \tag{14}$$

Thus, the relationship between RCS and θ_{di} has been established. According to the self-correlation and power spectrum functions of output voltage, it is possible to make a harmonic analysis in the frequency domain.

The power spectrum of the output voltage is the Fourier transform of its self-correlation function. And the self-correlation function of output voltage harmonic at an interval ε can be calculated by

$$\begin{aligned} R(\varepsilon) &= E\{|U_{1\max}|\cos[2\pi f_{\rm av}t + \theta_d(t)] \\ &\quad \times |U_{1\max}|\cos[2\pi f_{\rm av}(t+\varepsilon) + \theta_d(t+\varepsilon)]\} \\ &= \frac{|U_{1\max}|^2}{2}\cos(2\pi f_{\rm av}\varepsilon)E\{\cos[\theta_d(t+\varepsilon) - \theta_d(t)]\}. \end{aligned} \tag{15}$$

To make the items in the parentheses more concise, the expression can be replaced by

$$\theta_{\rm b}(t) = \theta_{\rm d}(t+\varepsilon) - \theta_{\rm d}(t). \tag{16}$$

It can be deduced from the central limit theorem that θ_{di} follows the normal distribution and so does θ_b. The probability density function is as follows:

$$p(\theta_b) = \frac{1}{\sqrt{2\pi}\theta_o\sqrt{1-\rho(\varepsilon)}} e^{\frac{-\theta_b^2}{2\theta_o^2[1-\rho(\varepsilon)]}}. \tag{17}$$

The substitution of (17) into (15) leads to the expression of the self-correlation function of $U_h(t)$ at an interval ε is

$$\begin{aligned} R(\varepsilon) &= \frac{1}{2}|U_{1\max}|^2\cos(2\pi f_{\rm av}\varepsilon)\int_{-\infty}^{+\infty} p(\theta_b)\cos(\theta_b)d\theta_b \\ &= \frac{1}{2}|U_{1\max}|^2\cos(2\pi f_{\rm av}\varepsilon)e^{-\theta_o^2[1-\rho(\varepsilon)]} \\ &= \frac{1}{2}|U_{1\max}|^2\cos(2\pi f_{\rm av}\varepsilon)e^{-\theta_o^2(\frac{3|\varepsilon|}{T} - \frac{3|\varepsilon|^2}{T^2})}. \end{aligned} \tag{18}$$

The power spectrum of $U_h(t)$ is the Fourier transform of (18).

Compared with ε, the variance of θ_{di} is large. In addition, the value of ε is relatively small, and $|\varepsilon|^2$ is a high-order infinitesimal. Therefore, the index item can be approximated to $\mathrm{e}^{-\theta_o^2\frac{3|\varepsilon|}{T}}$.

The Fourier transform of $\cos(2\pi f_{\rm av}\varepsilon)$ in (15) is as follows:

$$\mathcal{F}[\cos(2\pi f_{\rm av}\varepsilon)] = \pi[\delta(2\pi f - 2\pi f_{\rm av}\varepsilon) + \delta(2\pi f + 2\pi f_{\rm av}\varepsilon)] \tag{19}$$

where $\delta(f)$ is the unit pulse function, i.e., $\cos(2\pi f_{\rm av}\varepsilon)$ serves the function of shifting the rest of (18) to other frequency points in the frequency domain.

The Fourier transform of $\mathrm{e}^{-\theta_o^2\frac{3|\varepsilon|}{T}}$ in (18) is

$$\mathcal{F}[e^{-\theta_o^2\frac{3|\varepsilon|}{T}}] = \frac{6T\theta_o^2}{9\theta_o^4 + T^2\omega^2}. \tag{20}$$

As a result, the expression of the power spectrum corresponding to (18) can be written as

$$\begin{aligned} P(f) &= \frac{3\pi T|U_{1\max}|^2\theta_o^2}{9\theta_o^4 + 4\pi^2T^2(f \pm f_{\rm av})^2} \\ &= \frac{\pi T|U_{1\max}|^2}{3\theta_o^2}\frac{1}{1 + \frac{4\pi^2T^2}{9\theta_o^4}(f \pm f_{\rm av})^2}. \end{aligned} \tag{21}$$

Being negative, frequency is not of engineering significance, so there is only a need for paying attention to the frequency, which is positive in (21). The power spectrum is rewritten as

$$\begin{aligned} P(f) &= \frac{3\pi T|U_{1\max}|^2\theta_o^2}{9\theta_o^4 + 4\pi^2T^2(f - f_{\rm av})^2} \\ &= \frac{\pi T|U_{1\max}|^2}{3\theta_o^2}\frac{1}{1 + \frac{4\pi^2T^2}{9\theta_o^4}(f - f_{\rm av})^2}. \end{aligned} \tag{22}$$

In RSPWM, harmonics are centro-symmetrically distributed at the carrier frequency and its multiples. As for half of the 3-dB bandwidth of the harmonic power spectrum is

$$b_3' = f - f_{\rm av}. \tag{23}$$

Then,

$$\frac{\pi T|U_{1\max}|^2}{6\theta_o^2} = \frac{\pi T|U_{1\max}|^2}{3\theta_o^2}\frac{1}{1 + \frac{4\pi^2T^2}{9\theta_o^4}(f - f_{\rm av})^2}. \tag{24}$$

The 3-dB bandwidth of the harmonic power spectrum is represented as b_{31}, whose equation is

$$\begin{aligned} b_{31} &= 2b_{3'} \\ &= \frac{3}{\pi T}\theta_o^2. \end{aligned} \tag{25}$$

The abovementioned 3-dB bandwidth derivation is concerned with $n = 1$. Other bandwidths of harmonic power spectra can be calculated similarly as abovementioned. For example, when

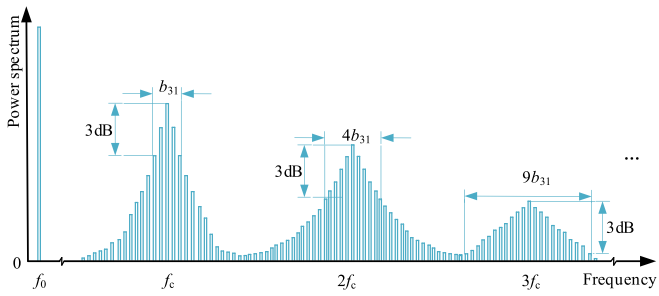

Fig. 5. 3-dB bandwidth of the harmonics' power spectrum.

$n = 2$, the random phase difference, calculated by (6) is twice that when $n = 1$, and the other variable values are the same. Thus, the variance of θ_{di} is four times that when $n = 1$. That means 3-dB bandwidth is four times that when $n = 1$. All the bandwidths can be calculated in a similar way.

According to (25), 3-dB bandwidth of harmonics power spectrum can be shown as Fig. 5. The harmonic power spectrum has a much wider bandwidth in the high-frequency band and its spectral lines will spread to the lower frequency band, in which the spectral lines are uplifted.

In the research on RSPWM, it is very important to select the probability statistical parameters of RCS. In [3], a qualitative analysis of the influence of RCS on the harmonic frequency domain distribution was made. From the perspective of frequency spectrum shift, the characters of RSPWM were also considered. It indicates that the maximum random carrier frequency is twice the value of switching frequency. The harmonic power spectrum is shown in Fig. 3, in which the random carrier frequency ranges from 0 to $2f_c$ when RCS is subject to the uniform distribution.

B. Random Slope PWM Based on Uniform Distribution

In this section, the power spectrum of RSPWM with the RCS in uniform distribution will be theoretically derived and calculated, which provides a theoretical basis for selecting the statistical parameters of RCS.

According to the characteristics of probability statistical parameters for different types of random distribution, the average value and variance of RCS can be determined when its frequency change range is fixed.

Considering that RCS is subject to uniform distribution and the carrier frequency ranges from $f_{\min}$ to $f_{\max}$, the mean carrier frequency of RCS based on uniform distribution is expressed as

$$f_{av} = \frac{f_{\max} + f_{\min}}{2}. \tag{26}$$

The variance of RCS is

$$f_o{}^2 = \frac{(f_{\max} - f_{\min})^2}{12}. \tag{27}$$

When $T_i = 1/f_i$, the probability density function of the random carrier period is expressed as

$$p(T_i) = \frac{1}{f_{\max} - f_{\min}} \left| \frac{1}{T_i{}^2} \right|. \tag{28}$$

From (28), the expectation value of RCS can be obtained, as shown in

$$\begin{aligned} E(T_i) &= \int_{\frac{1}{f_{\max}}}^{\frac{1}{f_{\min}}} \frac{T_i}{f_{\max} - f_{\min}} \left| \frac{1}{T_i{}^2} \right| dT_i \\ &= \frac{\ln f_{\max} - \ln f_{\min}}{f_{\max} - f_{\min}}. \end{aligned} \tag{29}$$

And the variance of RCS can be derived from the following formula:

$$\begin{aligned} T_o{}^2 &= \int_{\frac{1}{f_{\max}}}^{\frac{1}{f_{\min}}} T_i{}^2 p(T_i) dT_i - [E(T_i)]^2 \\ &= \int_{\frac{1}{f_{\max}}}^{\frac{1}{f_{\min}}} \left(\frac{T_i{}^2}{f_{\max} - f_{\min}} f_i^2 \right) dT_i - \left(\frac{\ln f_{\max} - \ln f_{\min}}{f_{\max} - f_{\min}} \right)^2 \\ &= \frac{1}{f_{\max} f_{\min}} - \left(\frac{\ln f_{\max} - \ln f_{\min}}{f_{\max} - f_{\min}} \right)^2. \end{aligned} \tag{30}$$

According to (14), the variance of θ_{di} is expressed as

$$\theta_o^2 = \frac{2\pi^2 f_{\text{av}}^3 T}{3} \left[\frac{1}{f_{\max} f_{\min}} - \left(\frac{\ln f_{\max} - \ln f_{\min}}{f_{\max} - f_{\min}} \right)^2 \right]. \tag{31}$$

When $n = 1$, the 3-dB bandwidth can be expressed as

$$b_{31} = 2\pi f_{\text{av}}^3 \left[\frac{1}{f_{\max} f_{\min}} - \left(\frac{\ln f_{\max} - \ln f_{\min}}{f_{\max} - f_{\min}} \right)^2 \right]. \tag{32}$$

From (32), it is known that 3-dB bandwidth is not linear with the random carrier frequency range, but is directly proportional to the variance θ_o^2 shown in (25). Meanwhile, θ_o^2 is determined when the random carrier frequency range is fixed under the condition of uniform distribution.

Obviously, the abovementioned theoretical deduction leads to the establishment of the relationship between probability statistical parameters of RCS and harmonics distribution in the frequency domain.

III. Simulation and Experiment

In simulation and experiment, the average frequency of the random carrier sequence is 5 kHz. According to the basic law of uniform distribution, the frequency range of RCS should be set in the range from 0 to 10 000 Hz. *N* is defined as the ratio of 3-dB bandwidth and twice the average carrier frequency.

TABLE I
PARAMETERS CORRESPONDING TO THE RANDOM CARRIER SEQUENCES

Sequence	N	T_o^2	b_{31}(Hz)
S_1	0.1	1.27×10^{-9}	1000
S_2	0.2	2.55×10^{-9}	2000
S_3	0.3	3.82×10^{-9}	3000
S_4	0.4	5.09×10^{-9}	4000
S_5	0.5	6.37×10^{-9}	5000
S_6	0.6	7.64×10^{-9}	6000
S_7	0.7	8.91×10^{-9}	7000
S_8	0.8	1.02×10^{-8}	8000
S_9	0.9	1.45×10^{-8}	9000

N is divided into ten segments and nine spacing points are taken to form nine random carrier sequences.

The main parameters of the random carrier sequences are listed in Table I. The parameters in Table I are calculated by the derivation.

In the same simulation and experiment conditions, the modulation depth is set as 0.8, the fundamental frequency as 50 Hz, and the repeated random period as 0.512 s (512 random carrier waves included). To make a comparison between FCPWM and RSPWM, a fixed carrier sequence whose frequency is 5 kHz is selected for FCPWM. The random sequences S_2, S_4, S_6, and S_8 are chosen for RSPWM in simulation and experiment. A purely resistive load has been used for simulation and experiment.

The power spectra of output voltage obtained in simulation are shown in Fig. 6(a)–(e).

As shown in Fig. 6, the peaks of harmonics power spectra are no longer concentrated at the carrier frequency and its multiple frequencies after the random RCS is used. RSPWM can make the output voltage smoother in the whole frequency domain than FCPWM. Besides, harmonic peaks of power spectra become less and less as the T_o^2 increases.

The power spectra in Fig. 6(c) are scattered more, compared with those peaks in Fig. 6(a) and (b) at 5 kHz, that is to say, the value of T_o^2 is large enough to scatter the peaks. But it can also be found that the power spectrum curve begins to rise when the frequency is lower than 5 kHz.

At the same time, a test platform mainly consisting of a 35-kW inverter, and a recorder is used for experiment and analysis. The inverter and other equipment are shown in Fig. 7(a). The block diagram in Fig. 7(b) shows the structure of the test platform. Set all the variables in the platform to be the same as those in the simulation. The modulation wave is stored in the DSP. The fixed carrier sequence and random carrier sequences are all generated by the computer and then stored in the ROM of the FPGA. And the switching driving signal is produced in the FPGA as well.

As shown in Fig. 8, the power spectra in the experiment are similar to that in the simulation. The peaks in FCPWM are no longer accumulated at 5 kHz and its multiples when RSPWM is used. At the same time, T_o^2 plays an important role in the harmonic's distribution. The FFT corresponding to Fig. 8 is shown in Fig. 9, which gives more detailed information about harmonics distribution in the frequency domain.

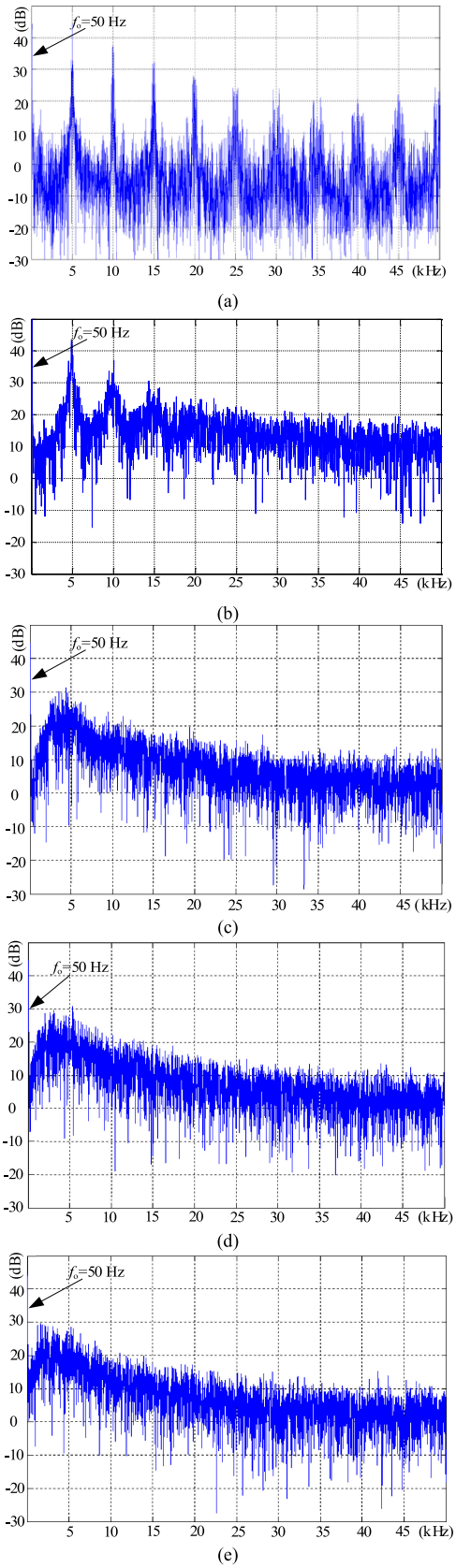

Fig. 6. Power spectra of output voltage in simulation. (a) $T_g^2 = 0$ (FCPWM). (b) $T_o^2 = 2.55 \times 10^{-9}$. (c) $T_o^2 = 5.09 \times 10^{-9}$. (d) $T_o^2 = 7.64 \times 10^{-9}$. (e) $T_o^2 = 1.02 \times 10^{-8}$.

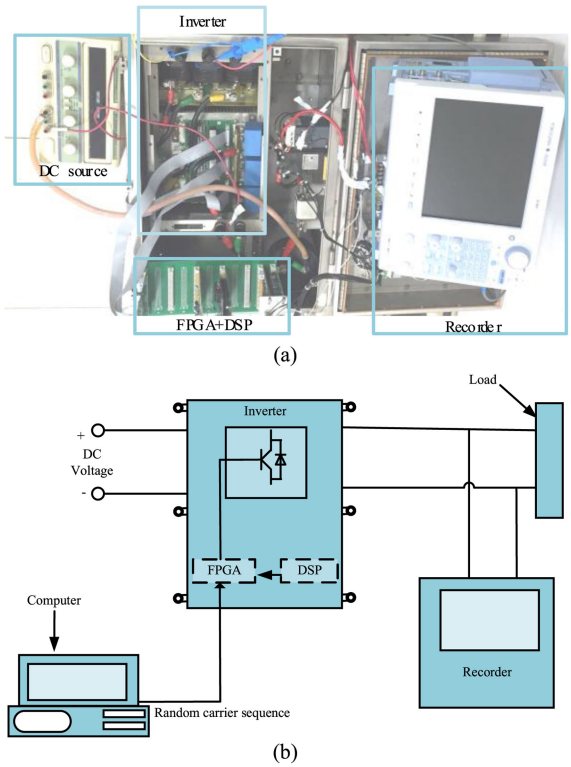

Fig. 7. 35 kW inverter for the experiment.

Fig. 9 shows the specific distribution of harmonic peaks and presents the following points.

1) Obvious harmonic peaks remain at 5 kHz and 10 kHz when the value of T_o^2 is 3.40×10^{-9}. That is because the variance of RCS is too small to disperse the harmonics.
2) With the increase of T_o^2, 3-dB bandwidth of the power spectrum becomes wider and wider, which leads to a more uniform distribution of harmonics in the frequency domain. In Fig. 9(b)–(e), there are not obvious harmonic peaks anymore.
3) From Fig. 9(e), it is seen that much more spectral lines are concentrated between 0 and 5 kHz due to the excessive variance of RCS, the blended lapping of multiple harmonic corresponding to 3-dB bandwidth in the whole frequency domain and the spreading of spectral lines in the high-frequency band to the low-frequency band.

It is worthy to note that the THD in Fig. 9(a)–(e) are almost the same. This is because RSPWM can disperse the harmonic but not eliminate it. And the variance of RCS that is too low or too high is not beneficial to the dispersion of harmonics. This is because harmonics are centro-symmetrically distributed at the carrier and its multiple frequencies. And the spectral lines in the high-frequency band are easily spread to the low-frequency band to uplift the lines in the low-frequency band. On the other hand, the harmonic peaks around 5 kHz are much higher than those in the high-frequency band. Even though the variance of RCS is increased, the spectra lines around 5 kHz are the densest. Therefore, the suggestion is that the ratio of 3-dB bandwidth to the twofold average carrier frequency be taken from 0.4 to 0.6.

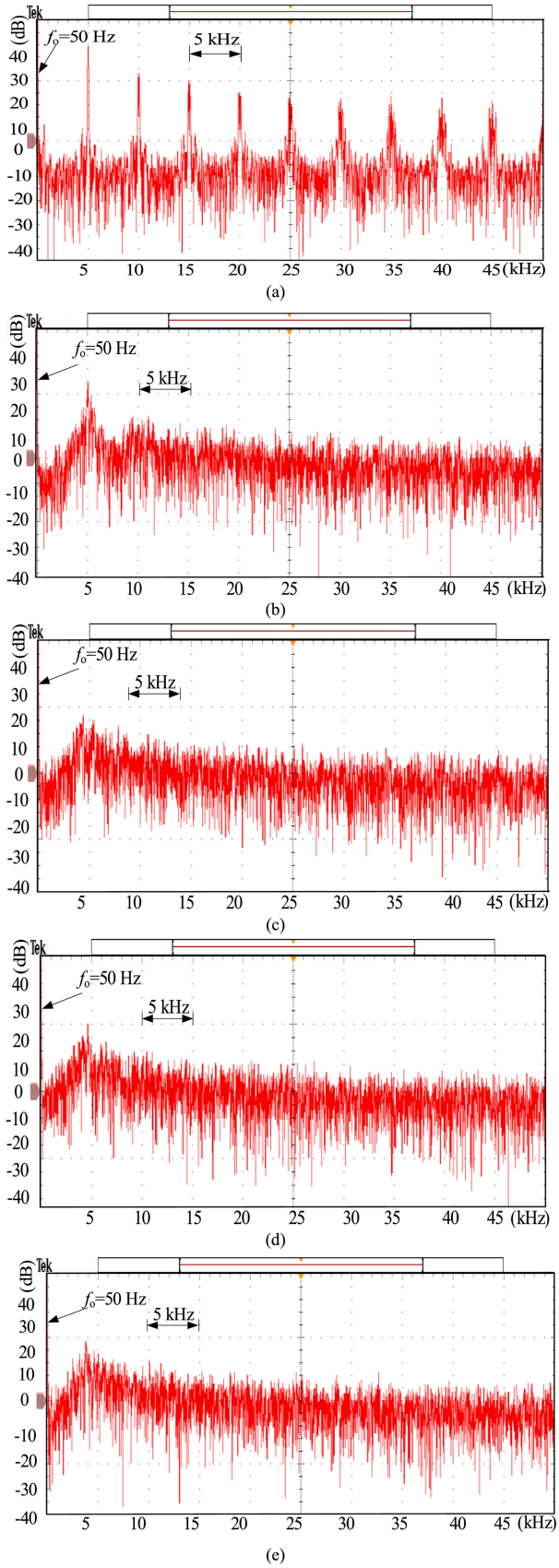

Fig. 8. Power spectra of output voltage in experiment. (a) $T_o^2 = 0$ (FCPWM). (b) $T_o^2 = 2.55 \times 10^{-9}$. (c) $T_o^2 = 5.09 \times 10^{-9}$. (d) $T_o^2 = 7.64 \times 10^{-9}$. (e) $T_o^2 = 1.02 \times 10^{-8}$.

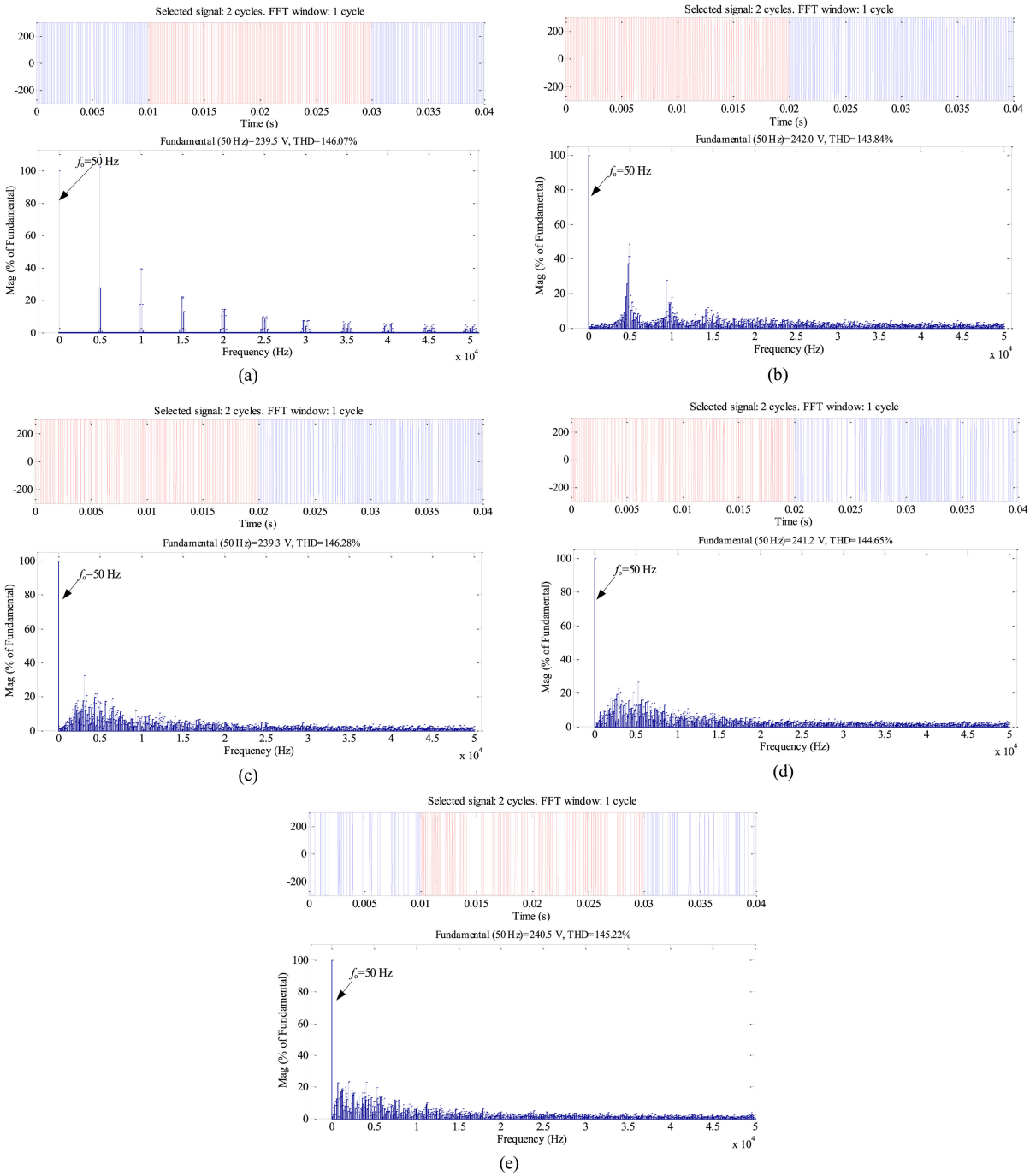

Fig. 9. Fast Fourier transform of output voltage. (a) $T_o^2 = 0$ (FCPWM). (b) $T_o^2 = 2.55 \times 10^{-9}$. (c) $T_o^2 = 5.09 \times 10^{-9}$. (d) $T_o^2 = 7.64 \times 10^{-9}$. (e) $T_o^2 = 1.02 \times 10^{-8}$.

IV. Conclusion

Based on RSPWM, this article has proposed a method of analyzing harmonic distribution in the frequency domain from the perspective of the power spectrum. Specifically, it includes choosing RCS subject to the uniform distribution, deducing the 3-dB bandwidth of the voltage harmonic power spectrum in RSPWM, and discovering the key variables affecting harmonic distribution. Simulations and experiments have been conducted in different conditions. According to the theoretical analysis of the RSPWM, an approach has been offered, which is used to select the main probability statistic parameters of RCS under the uniform distribution. Studies show that the proposed method is feasible and effective.

References

[1] P. N. Reddy, J. Amarnath, and P. L. Reddy, "Space vector based dual zero-vector random centered distribution PWM algorithm for direct torque control of induction motor drive for reduced acoustical noise," *Control Theory Informat.*, vol. 4, no. 2, pp. 14–28, 2011.

[2] J. L. Besnerais, V. Lanfranchi, M. Hecquet, and P. Brochet, "Characterization and reduction of audible magnetic noise due to PWM supply in induction machines," *IEEE Trans. Ind. Electron.*, vol. 57, no. 4, pp. 1288–1295, Apr. 2010.
[3] J. Xu, Z. Nie, and J. Zhu, "A random slope PWM with low electromagnetic interference," *Proc. CSEE*, vol. 37, no. 14, pp. 4175–4183, 2017.
[4] V. Jayamala, S. Ramasamy, and S. Jeevananthan, "Investigation of pseudorandom carrier pulse width modulation technique for induction motor drives," *2011 Nirma Univ. Int. Conf. Eng.*, Ahmedabad, Gujarat, Dec. 2011, pp. 1–5.
[5] A. M. Trzynadlowski, M. Andrzej, L. Stanislawlegowski, and R. L. Kirlin, "Random pulse-width modulation technique for voltage-controlled power inverters," *Int. J. Electron.*, vol. 68, no. 6, pp. 1027–1037, 1990.
[6] R. L. Kirlin, C. Lascu, and A. M. Trzynadlowski, "Shaping the noise spectrum in power electronic converters," *IEEE Trans. Ind. Electron.*, vol. 58, no. 7, pp. 2780–2788, Jul. 2011.
[7] A. M. Trzynadlowski, Z. Wang, J. M. Nagashima, C. Stancu, and M. H. Zelechowski, "Comparative investigation of PWM techniques for a new drive for electric vehicles," *IEEE Trans. Ind. Electron.*, vol. 39, no. 5, pp. 1396–1403, 2005.
[8] K. E. K. Drissi, P. C. K. Luk, B. Wang, and J. Fontaine, "Effects of symmetric distribution laws on spectral power density in randomized PWM," *IEEE Power Electron. Lett.*, vol. 1, no. 2, pp. 41–44, Sep./Oct. 2003.
[9] F. M. Ma, Z. G. Wu, and Y. M. Li, "Analysis and design of the random frequency PWM inverters," *Proc. CSEE*, vol. 28, no. 15, pp. 27–71, 2008.
[10] Y. C. Lim, Y. G. Jung, S. Y. Oh, and J. G. Kim, "A two-phase separately randomized pulse position PWM (SRP-PWM) scheme with low switching noise characteristics over the entire modulation index," *IEEE Trans. Power Electron.*, vol. 27, no. 1, pp. 362–369, Jan. 2012.
[11] K. K. Tse, S. H. Chung, S. Y. Huo, and H. C. So, "Analysis and spectral characteristics of a spread-spectrum technique for conducted EMI suppression," *IEEE Trans. Power Electron.*, vol. 15, no. 2, pp. 399–410, Mar. 2000.
[12] Z. G. Yin, Y. R. Zhong, and J. Liu, " Random PWM control technology of frequency control system based on Markov chain," *Electric Mach. Control*, vol. 14, no. 2, pp. 41–46, 2010.
[13] J. Xu, Z. Nie, and J. Zhu, "An optimal random carrier pulse width modulation technique based on a genetic algorithm," *J. Power Electron.*, vol. 17, no. 2, pp. 380–388, 2017.
[14] G. Marsala and A. Ragusa, "Spread spectrum in random PWM DC-DC converters by PSO&GA optimized randomness levels," in *Proc. IEEE 5th Int. Symp. Electromagn. Compat.*, 2017, pp. 1–6.
[15] J. Xu, Z. Nie, and J. Zhu, "Restudy on the random pulse width modulation," *Electric Mach. Control Appl.*, vol. 43, no. 6, pp. 45–51, 2016.
[16] L. Mathe, F. Lungeanu, D. Sera, P. O. Rasmussen, and J. K. Pedersen, "Spread spectrum modulation by using asymmetric-carrier random PWM," *IEEE Trans. Ind. Electron.*, vol. 59, no. 10, pp. 3710–3718, Oct. 2012.
[17] B. Liang, K. X. Wei, and Y. J. Yue, "Prediction of the conducted EMI in PWM converter system with parasitic parameters considered," *Sci. China Technological Sci.*, vol. 55, no. 10, pp. 2829–2836, 2012.
[18] S. Kaboli, J. Mahdavi, and A. Agah, "Application of random PWM technique for reducing the conducted electromagnetic emissions in active filters," *IEEE Trans. Ind. Electron.*, vol. 54, no. 4, pp. 2333–2343, Aug. 2007.
[19] S. R. Bowes and B. M. Bird, "Novel approach to the analysis and synthesis of modulation processes in power converters," in *Proc. Institution Elect. Eng.*, 1975.
[20] Z. K. Song and D. V. Sarwate, *The Frequency Spectrum of Pulse Width Modulated Signals*. Amsterdam, The Netherlands: Elsevier, 2003.
[21] L. F. Yakov and Alex Ruderman, "Discussion of a variable switching frequency PWM technique for induction motor drive to spread acoustic noise spectrum with reduced current ripple," *IEEE Trans. Ind. Appl.*, vol. 52, no. 6, p. 5355, 2016.
[22] A. C. B. Kumar and G. Narayanan, "Variable-switching frequency PWM technique for induction motor drive to spread acoustic noise spectrum with reduced current ripple," *IEEE Trans. Ind. Appl.*, vol. 52, no. 6, pp. 3927–3938, Sep./Oct. 2016.
[23] H. W. B. Vander and H. C. Skudelny, "Analysis and realization of a pulse width modulator based on voltage space vectors," *IEEE Trans. Ind. Appl.*, vol. 24, no. 1, pp. 142–150, Jan./Feb. 1988.
[24] A. Ruderman, B. Reznikov, and S. M. Busquets, "Asymptotic time domain evaluation of a multilevel multiphase PWM converter voltage quality," *IEEE Trans. Ind. Electron.*, vol. 60, no. 5, pp. 1999–2009, May 2013.
[25] K. L. Shi and H. Li, "Optimized PWM strategy based on genetic algorithms," *IEEE Trans. Ind. Electron.*, vol. 52, no. 5, pp. 1458–1461, Oct. 2005.
[26] A. G. Ruiz, M. J. G. Meco, F. H. Pérez, F. M. Vargas, and J. R. L. Heredia, "Reducing acoustic noise radiated by inverter-fed induction motors controlled by a new PWM strategy," *IEEE Trans. Ind. Electron.*, vol. 57, no. 1, pp. 228–236, Jan. 2010.
[27] Y. Huang, Y. Xu, W. Zhang, and J. Zou, "Hybrid RPWM technique based on modified SVPWM to reduce the PWM acoustic noise," *IEEE Trans. Power Electron.*, vol. 34, no. 6, pp. 5667–5674, Jun. 2019.
[28] R. Gamoudi, D. E. Chariag, and L. Sbita, "A review of spread-spectrum -based PWM techniques— a novel fast digital implementation," *IEEE Trans. Power Electron.*, vol. 33, no. 12, pp. 10292–10307, Dec. 2018.
[29] A. Peyghambari, A. Dastfan, and A. Ahmadyfard, "Selective voltage noise cancellation in three-phase inverter using random SVPWM," *IEEE Trans. Power Electron.*, vol. 31, no. 6, pp. 4604–4610, Jun. 2016.
[30] Y. Lai and B. Chen, "New random PWM technique for a full-bridge dc/dc converter with harmonics intensity reduction and considering efficiency," *IEEE Trans. Power Electron.*, vol. 28, no. 11, pp. 5013–5023, Nov. 2013.
[31] H. Khan, E. Miliani, and K. E. K. Drissi, "Discontinuous random space vector modulation for electric drives: a digital approach," *IEEE Trans. Power Electron.*, vol. 27, no. 12, pp. 4944–4951, Dec. 2012.
[32] C. Guocheng, *Frequency Conversion Technology Based on PWM*, Beijing, China: Machinery Industry Press, 1998.
[33] D. Holmes and T. Lipo, *Pulse Width Modulation for Power Converters: Principles and Practice*. Hoboken, NJ, USA: Wiley, 2003.
[34] G. Rajesh and A. Ghosh, "Switching characterization of cascaded multilevel inverter controlled systems," *IEEE Trans. Ind. Electron.*, vol. 55, no. 3, pp. 1047–1058, Mar. 2008.
[35] O. Dordevic, M. Jones, and E. Levi, "Analytical formulas for phase voltage RMS squared and THD in PWM multiphase systems," *IEEE Trans. Power Electron.*, vol. 30, no. 3, pp. 1645–1656, Mar. 2015.

Jie Xu received the Ph.D. degree in electric engineering from the Specialized Electrical Research Institute of Science and Technology, Naval University of Engineering, Wuhan, China, in 2017.

He is currently a Research Assistant Professor with the Specialized Electrical Research Institute of Science and Technology, Naval University of Engineering. His main research interests include signal processing and power electronic technology.

Ziling Nie received the B.S. (hons.), M.S., and Ph.D. degrees from the Huazhong University of Science and Technology, Wuhan, China, in 1998, 2001, and 2005, respectively.

He was a Visiting Scholar with the University of Michigan, Ann Arbor, MI, USA, in 2007. He is currently a Professor with the Naval University of Engineering, Wuhan, China. His current research interests include power electronics, high-voltage andhigh-power converters, and HEV/EVs.

Junjie Zhu (Member, IEEE) received the B.S., M.S., and Ph.D. degrees in electrical engineering from the Naval University of Engineering, Wuhan, China, in 2007, 2009, and 2013, respectively.

He is currently an Assistant Professor with the Naval University of Engineering. His current research interests include power electronic converters, matrix converters, microgrids, distributed generation, and the application of power electronics in electromagnetic emissions.